# 4,4′-Bipyridazine: a new twist for the synthesis of coordination polymers†‡

**Konstantin V. Domasevitch,*[a] Il'ya A. Gural'skiy,[a] Pavlo V. Solntsev,[a] Eduard B. Rusanov,[b] Harald Krautscheid,[c] Judith A. K. Howard[d] and Alexander N. Chernega[b]**

***Received 15th March 2007, Accepted 20th April 2007***
***First published as an Advance Article on the web 9th May 2007***
**DOI: 10.1039/b703911e**



A new polydentate ligand 4,4′-bipyridazine (4,4′-*bpdz*) was prepared by employing inverse electron demand cycloaddition of 1,2,4,5-tetrazine. A unique combination of structural simplicity, ampolydentate character and efficient donor properties towards Cu(I), Cu(II) and Zn(II) provide wide new possibilities for the synthesis of coordination polymers incorporating the 4,4′-*bpdz* module either as a bi-, tri- or tetradentate connector between the metal ions. 1D coordination polymers $Cu_2$(4,4′-*bpdz*)$(CH_3CO_2)_4\cdot 4H_2O$ and Zn(4,4′-*bpdz*)$(NO_3)_2$, and interpenetrated (4,4)-nets in $[Cu$(4,4′-*bpdz*$)_2(H_2O)_2]S_2O_6$ were closely related to 4,4′-bipyridine compounds. 1D "ladder-like" polymer $Cu_2$(4,4′-*bpdz*$)_3(CF_3CO_2)_4$ and the unprecedented 3D binodal net ($\{8^6\}\{6^3;8^3\}$) in $[Cu_3$(4,4′-*bpdz*$)_6(H_2O)_4](BF_4)_6\cdot 6H_2O$ were based upon a combination of linear and angular organic bridges. Complex $[Cu_3(OH)_2$(4,4′-*bpdz*$)_3(H_2O)_2\{CF_3CO_2\}_2](CF_3CO_2)_2\cdot 2H_2O$ has a "NbO-like" 3D topology incorporating discrete dihydroxotricopper(II) clusters linked by tri- and tetradentate ligands. The tetradentate function of the 4,4′-*bpdz* ligand was especially relevant for copper(I) complexes, which adopt layered $Cu_2X_2$(4,4′-*bpdz*) (X = Cl, Br) or 3D chiral framework (X = I) structures based upon infinite $(CuX)_n$ chains. The electron deficient character of the ligand was manifested by short anion–π interactions (O–π 3.02–3.20; Cl–π 3.35 Å), which may be involved as a factor for controlling the supramolecular structure.

## Introduction

The design of novel bridging ligands attracts significant attention in view of their potential applications in framework coordination polymers.[1,2] Inherent functional and conformational properties of the ligands are commonly relevant for the connectivity within the entire structure and they could assist in the development of metal–organic frameworks in a rational fashion,[3,4] including synthesis of polynuclear systems, hybrid organic/inorganic materials and highly-connected frameworks incorporating metal cluster motifs. In this way, polydentate nitrogen donor ligands offer very efficient approaches for the design and fine-tuning of the structure and properties of coordination polymers, as revealed by examining metal complexes with different bifunctional azole ligands: 1,2,4-triazoles,[5] 4,4′-bipyrazole,[6] 4-pyridylpyrazole[7] and 4,4′-bitriazole.[8] Pyridazines, the most typical connectors for bridging between closely situated metal ions, may be expected to be especially rich and potentially versatile for the synthesis of coordination polymers. A variety of characteristic metal–pyridazine chains, helices[9] and polynuclear motifs[10] may be viewed as attractive structural prototypes for supramolecular synthesis of coordination arrays involving polyfunctional pyridazine ligands.

In this context, a paradigmatic prototype for the tectons bearing multiple pyridazine donor-N sites is provided by 4,4′-bipyridazine (Scheme 1), a structurally simple molecule combining the ability for interconnection of either closely separated or distal metal ions, efficient bridging of many metal centers and the ability to sustain different binding directions depending on the molecular conformations. From the crystal design perspective, 4,4′-bipyridazine may unite the potential of the parent monofunctional heterocycle, linear rod-like connectors of the 4,4′-bipyridine type, and many of the angular bridging ligands. Herein, we report very simple synthesis of this hitherto unknown ligand, coordination preferences of 4,4′-bipyridazine and its utility for generation of extended coordination polymers.

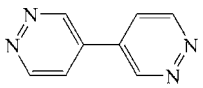

*(4,4′-bpdz)*

**Scheme 1** 4,4′-Bipyridazine ligand explored in the present study.

## Results and discussion

In combination with transition metal ions 4,4′-bipyridazine acts as an efficient polydentate N-donor readily producing a variety of polymeric coordination architectures. The ligand revealed quite diverse and versatile structural functions, originating in the availability of two pairs of non-equivalent donor-N atoms

[a]*Inorganic Chemistry Department, Kiev University, Volodimirska Str.64, Kiev, 01033, Ukraine. E-mail: dk@univ.kiev.ua*
[b]*Institute of Organic Chemistry, Murmanskaya Str.4, Kiev, 253660, Ukraine*
[c]*Institut für Anorganische Chemie, Universität Leipzig, Linnéstraße 3, D-04103, Leipzig, Deutschland*
[d]*Dept. of Chemistry, University of Durham, Durham, UK DH1 3LE*

† The HTML version of this article has been enhanced with colour images.

‡ Electronic supplementary information (ESI) available: Detailed procedure for preparation of unsubstituted 1,2,4,5-tetrazine. See DOI: 10.1039/b703911e

 

and therefore 4,4′-bipyridazine can support the integrity of the coordination patterns either as a bi-, tri- or tetra-connected module (Scheme 2).

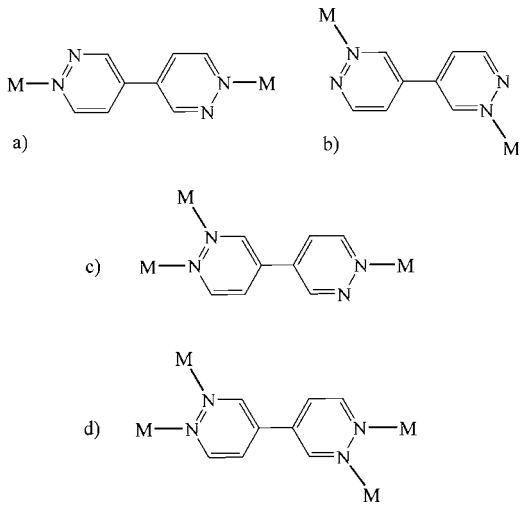


**Scheme 2** Ampolydentate properties of 4,4′-bipyridazine in metal complexes: (a) "4,4′-bipyridine like" coordination in structures **1–5**; (b) "3,3′-bipyridine like" coordination in **4**, **5**; (c) tridentate mode in **6**; (d) tetradentate mode in **6–9**.

In complexes with $Cu^{2+}$ and $Zn^{2+}$ ions the ligand was typically bidentate and thus it utilized only a half of the available coordination functionality. This is consistent with previous examinations of pyridazine itself that is coordinated monodentately in a number of $Cu^{2+}$ complexes, many of which are closely related to their pyridine analogs. Similarly, in some cases 4,4′-bipyridazine plays the role of a simple rod-like bitopic linker between pairs of metal ions separated by *ca.* 11 Å, as typically occurs for 4,4′-bipyridine bridges.

### Complexes related to 4,4′-bipyridine analogs

The "bipyridine-like function" of the ligand was best illustrated by 1D polymeric structures of $Cu_2(4,4'\text{-}bpdz)(CH_3CO_2)_4\cdot 4H_2O$ **1** and $Zn(4,4'\text{-}bpdz)(NO_3)_2$ **2**. Structure **1** is based upon typical centrosymmetric copper(II)/acetate dimers linked into linear chains employing the axial coordination positions at two metal ions (Fig. 1, Table 1). Such a pattern has an exact precedent in the chemistry of 4,4′-bipyridine in the structure of $Cu_2(4,4'\text{-}bipy)(CH_3CO_2)_4\cdot$DMF.[11] All Cu–O distances are uniform (1.963(1)–1.986(2) Å), while Cu–N separations were appreciably longer and actually the same as for the bipyridine analog (2.179(2) and 2.187(3) Å, respectively). The chains aggregate with extensive hydrogen bonding involving very rare discrete water tetramers (O–O 2.79, 2.82 Å),[12] and the interaction between the coordination portion and the water assemblies occurs *via* bifurcated weak hydrogen bonds, which engage non-coordinated pyridazine nitrogen atom as one of the hydrogen bond acceptors (O5–O3 3.056; O5–N2 3.278 Å, Fig. 1).

In the zinc complex $Zn(4,4'\text{-}bpdz)(NO_3)_2$ **2** the coordination mode of the ligand is identical: the metal ions were connected into zig-zag chains (N–Zn–N 103.51(6)°) and the coordination environment was completed with two bidentate nitrate groups (Zn–O 2.102(2)–2.329(2) Å) (Fig. 2, Table 1). The ligand adopts

**Table 1** Selected bond distances (Å) and angles (°) for complexes **1–3**

| | | | |
|---|---|---|---|
| $Cu_2(4,4'\text{-}bpdz)(CH_3CO_2)_4\cdot 4H_2O$ **1** (a: $-x$, $1-y$, $1-z$) | | | |
| Cu1–O1 | 1.986(2) | O3–Cu1–O1 | 89.19(7) |
| Cu1–O3 | 1.963(1) | O3–Cu1–N1 | 98.91(6) |
| Cu1–O2a | 1.978(2) | O1–Cu1–N1 | 96.52(7) |
| Cu1–O4a | 1.975(1) | O2a–Cu1–O1 | 168.40(6) |
| Cu1–N1 | 2.179(2) | N1–Cu1–Cu1a | 173.45(5) |
| Cu1–Cu1a | 2.6294(6) | | |
| $Zn(4,4'\text{-}bpdz)(NO_3)_2$ **2** (a: $0.5-x$, $0.5+y$, $1.5-z$) | | | |
| Zn1–N1 | 2.042(2) | N1–Zn1–N3a | 103.51(6) |
| Zn1–N3a | 2.044(2) | N1–Zn1–O2 | 97.44(6) |
| Zn1–O1 | 2.206(2) | N1–Zn1–O1 | 155.52(6) |
| Zn1–O2 | 2.102(2) | O4–Zn1–O1 | 84.97(8) |
| Zn1–O4 | 2.175(2) | O4–Zn1–O5 | 55.52(6) |
| Zn1–O5 | 2.329(2) | O2–Zn1–O1 | 58.95(6) |
| $[Cu(4,4'\text{-}bpdz)_2(H_2O)_2]S_2O_6$ **3** (a: $0.5-x$, $-0.5+y$, $-0.5+z$; b: $-0.5-x$, $0.5+y$, $0.5+z$). | | | |
| Cu1–N1 | 2.067(3) | N5–Cu1–N1 | 175.1(1) |
| Cu1–N5 | 2.049(3) | N7a–Cu1–N3b | 179.3(1) |
| Cu1–N3b | 2.047(3) | O1–Cu1–O2 | 177.8(1) |
| Cu1–N7a | 2.041(3) | N5–Cu1–O1 | 91.3(1) |
| Cu1–O1 | 2.272(3) | N1–Cu1–O1 | 93.6(1) |
| Cu1–O2 | 2.417(3) | N1–Cu1–O2 | 86.5(1) |

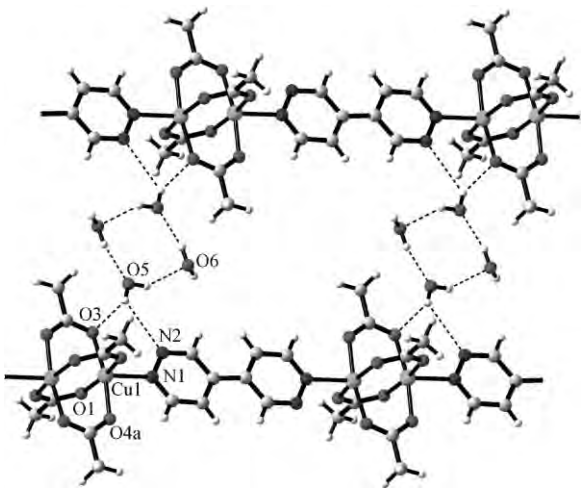


**Fig. 1** Structure of **1** involving linear coordination chains bridged by tetraaqua ensembles.

a twisted configuration (dihedral angle between two pyridazine cycles 44.54(7)°), while in the copper complex **1** the molecule was planar and centrosymmetric. Such a 1D chain shape bears a close resemblance with a polymer $Zn(4,4'\text{-}bipy)(NCS)_2$,[13] however, the structure of the nitrate analog is completely different since the metal ions coordinate the additional water molecules: $Zn(4,4'\text{-}bipy)(H_2O)_2(NO_3)_2$.[14]

It is likely that the organization of the structure **2** was greatly influenced by a set of specific interactions, which occur between the electronegative oxygen atoms and aromatic π-clouds (Fig. 2, b). Such anion–π stacking itself has very few recent literature precedents, all of which involve interactions with the most electron deficient heteroaromatic systems: 1,2,4,5-tetrazines,[15]

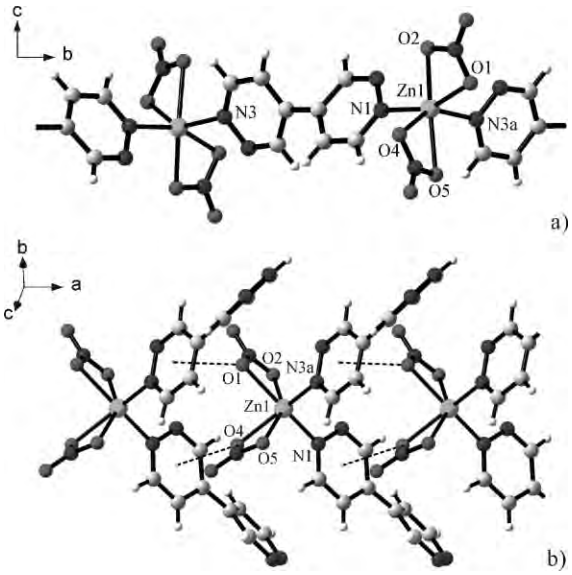


**Fig. 2** Two views of 1D zig-zag polymer **2**: (a) coordination chain formed by linear 4,4′-bipyridazine bridges, (b) the interchain interactions that occur by means of close anion–π stacking (O1···π 3.017(2); O4···π 2.948(2) Å).

1,3,5-triazines[16] and condensed pyridazino[4,5-*d*]pyridazine.[17] The nitrate oxygen atoms exhibit appreciably short contacts with the heterocyclic ring and appear nearly above the centroids of pyridazine cycles from the adjacent chains (O–centroid distances 2.95 and 3.02 Å; Table 2). Such an interaction of non-coordinated $NO_3^-$ anions (with the 1,3,5-triazine cycle) was even certainly weaker (O–π distances 3.20 Å).[16] This is the first observation of a pronounced anion–π binding with simple diazines, and it allows the postulation of special properties of the 4,4′-bipyridazine ligand compared with a 4,4′-bipyridine prototype.

Structure of the metal–organic framework in $[Cu(4,4'\text{-}bpdz)_2(H_2O)_2]S_2O_6$ **3** was also closely related to the very characteristic coordination archetypes provided by bitopic rod-like connectors. Metal ions coordinate four pyridazine nitrogen atoms (Cu–N 2.041(3)–2.067(3) Å) in the equatorial plane and two distal water molecules in the apical positions (Cu–O 2.272(3), 2.417(3) Å) and the coordination portion of the structure exists in the form of 2D (4,4)–net (Fig. 3). The latter provides rectangular meshes with inner cavities of *ca.* 6 × 6 Å size and interpenetrate with the identical (4,4)-nets situated orthogonally.[18] Similar ensembles of (4,4)-nets interpenetrated in a diagonal–diagonal fashion[19] was observed for related $[Cu(4,4'\text{-}bipy)_2(H_2O)_2]X$ (X = $SiF_6$, $GeF_6$,[20] $S_2O_6$[21]) complexes. The dithionate counter anions are situated in the channels provided by interpenetrated networks and held by a set of OH–O hydrogen bonds and anion–π stackings, which are comparable with the ones observed in structure **2** (O–π 3.018(4) Å, $\varphi$ 78.9°), and are shorter than O–π contacts in the 4,4′-bipyridine analog (3.23 Å).[21]

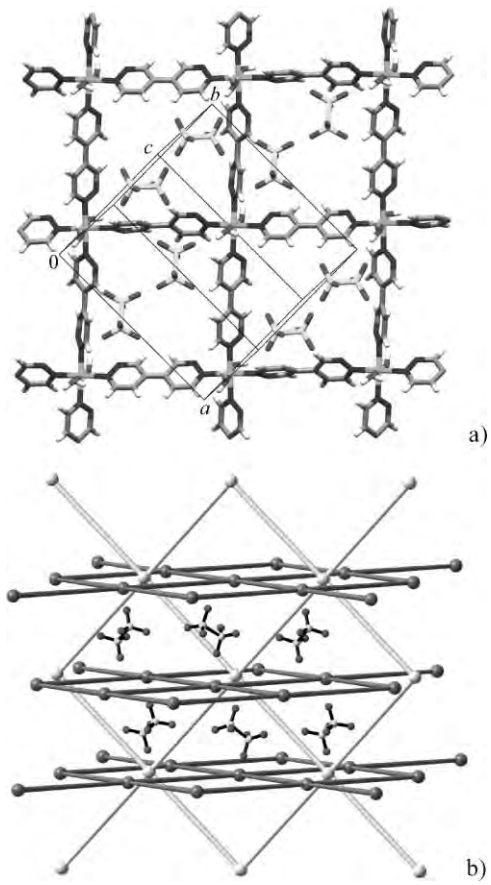


**Fig. 3** Structure of the square-grids coordination layer $[Cu(H_2O_2)(4,4'\text{-}bpdz)_2]_n$ in **3**, (a) with non-coordination dithionate anions situated inside the cages, (b) Diagonal–diagonal interpenetration of the coordination nets generating the 3D supramolecular structure.

### Structures with different coordination modes of the ligand

4,4′-Bipyridazine ligand offers even wider prospects for the synthesis of coordination frameworks as may be compared with the prototypal 4,4′-bipyridine. When coordinated *via* the pairs of $N^2$, $N^{2'}$ or $N^1N^{2'}$ nitrogen atoms, the organic module could be functionally equivalent to 3,3′- or 3,4′-bipyridines and the different bridging modes may coexist within a single coordination topology. In this respect the ligand can act as a "mixture of isomeric bipyridines" and such a combination could support unusual metal–organic connectivities.

Thus, complex $Cu_2(4,4'\text{-}bpdz)_3(CF_3CO_2)_4$ **4** (Fig. 4, Table 3) adopts a ladder-like motif based upon T-shape $CuN_3$ coordination.[3] Within the ladder, two linear $\{Cu(4,4'\text{-}bpdz)(CF_3CO_2)_2\}_n$

**Table 2** Geometry of the anion–π interactions in structure **2**

| Group | X[a] | X–C(N) range/Å | X···centroid distance/Å | X···plane distance/Å | $\varphi$/°[b] |
|---|---|---|---|---|---|
| N1N2C1C2C3C4 | O4a | 3.00–3.45 | 2.948(2) | 2.894(2) | 79.0 |
| N3N4C5C6C7C8 | O1b | 2.99–3.56 | 3.017(2) | 2.926(2) | 75.9 |

[a] Symmetry codes: a: $x-1$, $y$, $z$; b: $1.5-x$, $-0.5+y$, $1.5-z$. [b] Angle of the X–π axis to the plane of the aromatic cycle.

 

**Table 3** Selected bond distances (Å) and angles (°) for complexes **4–6**

| | | | |
|---|---|---|---|
| $Cu_2(4,4'\text{-}bpdz)_3(CF_3CO_2)_4$ **4** (a: $x, -1+y, z$) | | | |
| Cu1–O1 | 1.937(2) | O1–Cu1–O3 | 177.43(7) |
| Cu1–O3 | 1.989(2) | O1–Cu1–N3 | 91.80(8) |
| Cu1–N1 | 2.323(2) | O3–Cu1–N3 | 88.81(8) |
| Cu1–N3 | 2.026(2) | N3–Cu1–N5a | 171.62(8) |
| Cu1–N5a | 2.010(2) | N3–Cu1–N1 | 94.16(8) |
| $[Cu_3(H_2O)_4(4,4'\text{-}bpdz)_6(H_2O)_4](BF_4)_6\cdot 6H_2O$ **5** (a: $2-x, -y, 1-z$) | | | |
| Cu1–N1 | 2.000(3) × 2 | N1–Cu1–N3 | 88.1(1) |
| Cu1–N3 | 2.025(3) × 2 | N1–Cu1–N3a | 91.9(1) |
| Cu2–N5 | 2.019(3) | N5–Cu2–N7 | 92.4(1) |
| Cu2–N7 | 2.028(4) | N5–Cu2–N11 | 172.4(1) |
| Cu2–N9 | 2.051(4) | N5–Cu2–N9 | 89.1(1) |
| Cu2–N11 | 2.033(3) | N5–Cu2–O2 | 93.4(1) |
| Cu2–O2 | 2.347(4) | N7–Cu2–O2 | 90.8(2) |
| $[Cu_3(OH)_2(4,4'\text{-}bpdz)_3(H_2O)_2\{CF_3CO_2\}_2](CF_3CO_2)_2\cdot 2H_2O$ **6** (a: $0.5-x, 0.5-y, 1-z$; b: $-0.5+x, -0.5+y, z$) | | | |
| Cu1–O1 | 1.887(2) × 2 | O1–Cu1–N3 | 84.91(7) |
| Cu1–N1 | 2.340(3) × 2 | O1–Cu1–N1 | 93.10(8) |
| Cu1–N3 | 2.146(2) × 2 | N3–Cu1–N1 | 91.30(8) |
| Cu2–O1 | 1.883(2) | O1–Cu2–O2 | 171.5(1) |
| Cu2–O2 | 1.957(2) | N4–Cu2–N5b | 176.37(9) |
| Cu2–N2a | 2.459(2) | N4–Cu2–N2a | 88.25(9) |
| Cu2–N4 | 2.069(2) | O1–Cu2–N4 | 87.54(8) |
| Cu2–N5b | 2.008(2) | Cu2–O1–Cu1 | 118.23(9) |

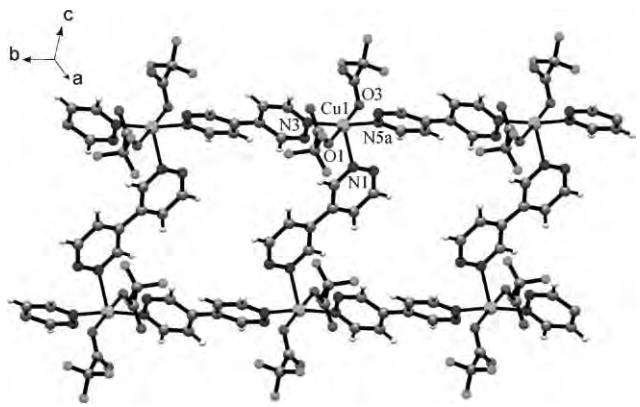


**Fig. 4** 1D "ladder-like" polymer **4** involving square-pyramidal coordination at the copper ions and two types of the bipyridazine bridges.

chains (Cu–Cu 10.98 Å) were supported by rod-like 4,4′-*bpdz* connectors, while cross-linking of the chains achieved by an additional set of the ligands, which were coordinated in a "3,3′-*bipy*" fashion (Cu–Cu 9.97 Å). This feature is essential for a minimization of inner volume of the resulting rectangular meshes.

The structure of $[Cu_3(4,4'\text{-}bpdz)_6(H_2O)_4](BF_4)_6\cdot 6H_2O$ **5** is much more complicated and the coexistence of the above linear and angular bipyridazine bridges (in a 1 : 1 proportion) clearly contributes to the very unusual framework topology. Two unique copper(II) ions adopt a similar 4 + 2 octahedral coordination, with four nitrogen atoms situated in the equatorial plane (Cu–N 2.00–2.05 Å, Table 3) and two distal aqua ligands in the apical positions (Fig. 5). One of the water molecules is bridging between the two copper ions, with very lengthy Cu–O distances of 2.48 and 2.58 Å, and this unites the coordination centers into "trimers". Copper–

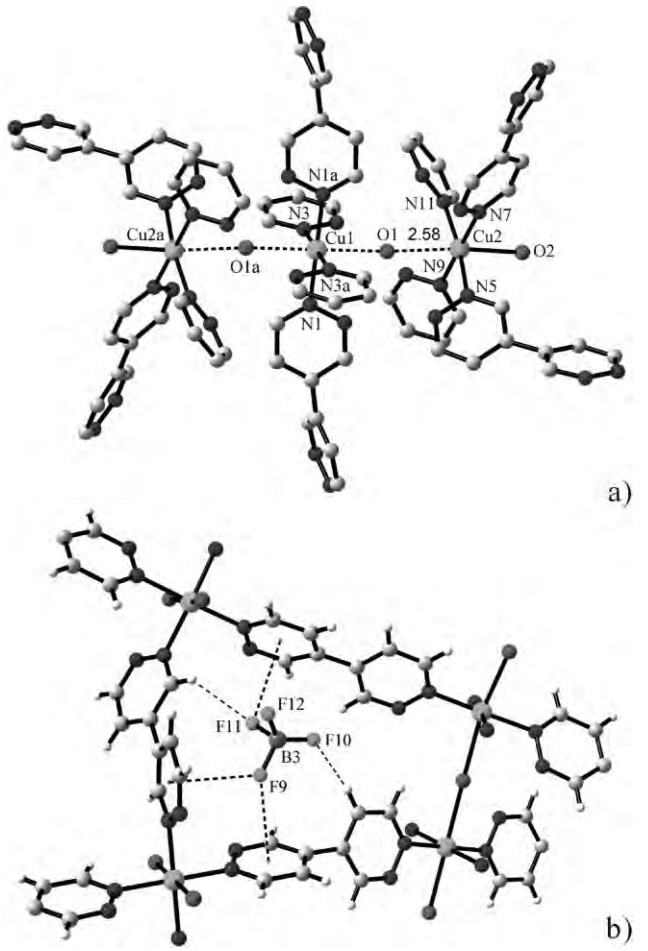


**Fig. 5** (a) Trinuclear coordination unit in structure **5** supported by two weak aqua bridges, (b) Situation of $BF_4^-$ anion inside the crystal cage and its interaction with the ligand frames by CH–F hydrogen bonding and anion–π stackings (F9 · · · π 3.05, 3.14; F11 · · · π 3.27 Å).

bipyridazine connectivity is an unprecedented 3D binodal four-connected net based upon two kinds of the vertices, which differ in the coordination sequences: 4, 12, 36, 78... for Cu1; and 4, 12, 33, 73... for Cu2 (total Schläfli symbol $\{8^6\}\{6^3;8^3\}$) (Fig. 6). Each "copper trimer" coordinates twelve bipyridazine molecules and is linked to eight equivalent closest neighbors (half of the links represented by pairs of the organic ligands), and when considering the trimeric units as augmented net nodes, the overall 3D topology may be regarded as an eight-connected primitive hexagonal net (Schläfli symbol $\{3^6;4^{18};5^3;6\}$) (Fig. 6). Non-coordinated anions are involved in hydrogen bonding with the water molecules and also in extensive CH–F and anion–π bonding with the coordination framework. It allows the postulation of a certain templating effect of tetrafluoroborate anions for stabilization of small crystal cavities as depicted in Fig. 5(b). Surprisingly, atom F9 interacts with two pyridazine cycles simultaneously, with short F–π (centroid) separations (3.05 and 3.14 Å).

### Structures involving 1,2-pyridazine bridges

Partial utilization of the ligand donor-N functionality in complexes **1–5** is a clear consequence of the inherent electron deficient character of the pyridazine cycle, the factor mitigating against the

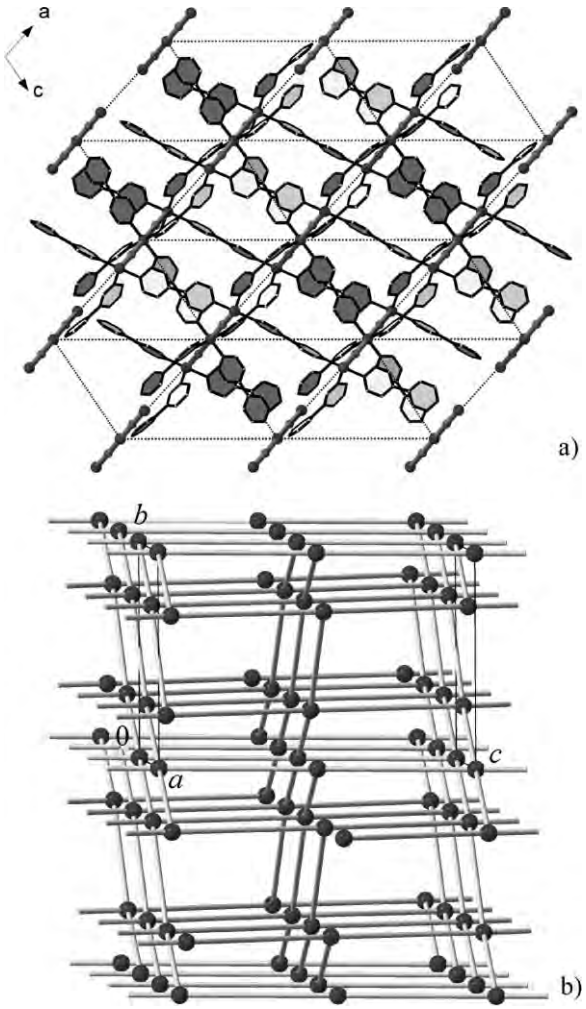


**Fig. 6** (a) Fragment of the structure of **5**, showing the scheme for connection of the tricopper units to the six closest neighbors. Two additional links occur in the axial directions leading to the generation of a primitive hexagonal lattice (*hex*); (b) Overall 3D metal–bipyridazine linkage in the form of a four-connected binodal $\{8^6\}\{6^3;8^3\}$ net.

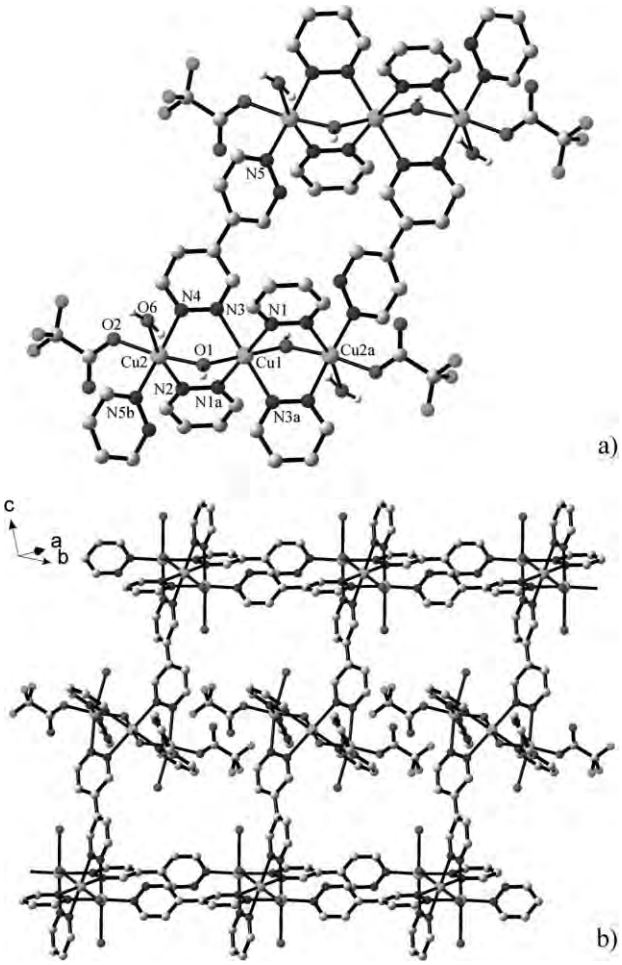


**Fig. 7** (a) Finite dihydroxotricopper(II) ensembles sustaining vertices of the framework in **6**. Note that the trinuclear unit accommodates four 1,2-diazine bridges and two monodentate pyridazine cycles, (b) Interconnection of the tricopper clusters by combination of three- and tetradentate 4,4′-*bpdz* ligands leading to a 3D "NbO-like" four-connected topology.

coordination of the ligand to many metal ions. However, higher donor capacity of the 4,4′-bipyridazine module may be anticipated for the systems involving small inorganic bridges (such as μ-chloro, μ-hydroxo) that could assist in interconnection of closely separated metal ions and formation of 1,2-diazine bridges.[10,17] In this case 4,4′-bipyridazine may provide either tri- or tetradentate coordination modes, which offer a special potential from the design perspective.

Thus a partial hydrolysis in aqueous solution (see Experimental) led to crystallization of the hydroxopolymer $[Cu_3(OH)_2(4,4'\text{-}bpdz)_3(H_2O)_2\{CF_3CO_2\}_2](CF_3CO_2)_2\cdot 2H_2O$ **6**. The structure was based upon finite dihydroxotricopper(II) units allowing accommodation of four 1,2-diazine bridges and two additional pyridazine groups were coordinated monodentately (Fig. 7, Table 3). Accordingly, the polymeric structure was generated by a combination of tri- and tetradentate 4,4′-bipyridazine molecules (in a 2 : 1 proportion), which connect each of the tricopper units to four closest neighbors. In this way, pairs of antiparallel tridentate ligands assemble the clusters into the chains and the tetradentate bridges extend this motif in the orthogonal direction (Fig. 7). The entire framework adopts a four-connected 3D topology, which is commonly related to the NbO structure and incorporates the tricopper units as an origin of the net connectivity.

This coordination motif has a precedent in the chemistry of parent pyridazine[10] and formation of the complicated framework incorporating trinuclear nodes in **6** is itself very illustrative for the general principles of crystal design. In the hydroxocluster, the central copper ion has a distorted octahedral environment with appreciably short Cu–OH bonds (1.887(2) Å) and two kinds of Cu–N bonds (2.146(2) and 2.340(3) Å). Metal–hydroxo bonds were also found to be the shortest separations within the typically distorted 4 + 2 coordination octahedron of two outer copper ions, while the axial positions were occupied by the distal aqua ligand (2.669 Å) and pyridazine-N donor (2.459 Å).

The tetradentate function of the ligand may be even more characteristic and predictable for the extremely soft acids (such as $Cu^+$ or $Ag^+$) favoring efficient back-bonding and coordination to unsaturated N atoms. In this context we have examined copper(I) chloride, bromide and iodide, as a system allowing the rational design of coordination topology by hybrid organic/inorganic

 

interconnection of the metal ions with μ-halide and 1,2-diazine bridges.

Isostructural complexes $Cu_2X_2$(4,4′-*bpdz*) (X = Cl **7**, Br **8**) adopt 2D polymeric arrays integrating infinite $(CuX)_n$ chains (Fig. 8, Table 4). Along the chain, each pair of metal ions are bridged by pyridazine and thus sets of tetradentate 4,4′-bipyridazine ligands provide pairwise interconnection of the inorganic chains into the layers. This pattern has no direct analogy in the chemistry of the parent heterocycle itself. All known copper(I) chloride and bromide complexes with pyridazine involve $Cu_2X_2$ rhombes as basic elements of the structure,[22] while a very comparable chain-like motif was characteristic for bulky diazines such as 2,3-diazabicyclo(2.2.1)hept-2-ene[23] and 1,2,3,6,7,8-hexahydro-cinnolino[5,4,3-*cde*]cinnoline.[24] However, orientation of the pyridazine bridges along the coordination chains in **7** and **8** is very specific and it facilitates steric accessibility of the chlorine (bromine) atoms, which are in close contact with the aromatic–π frames from the adjacent layer (Cl–π 3.347; Br–π 3.473 Å) (Fig. 8(b)). These parameters only slightly exceed separations for the recently documented chloride–π stacking with the electron deficient 1,3,5-triazine cycle (3.20 Å).[25] Such a type of interaction could be regarded as very characteristic for the 4,4′-bipyridazine ligand and it contributes to the controlling of the framework structure.

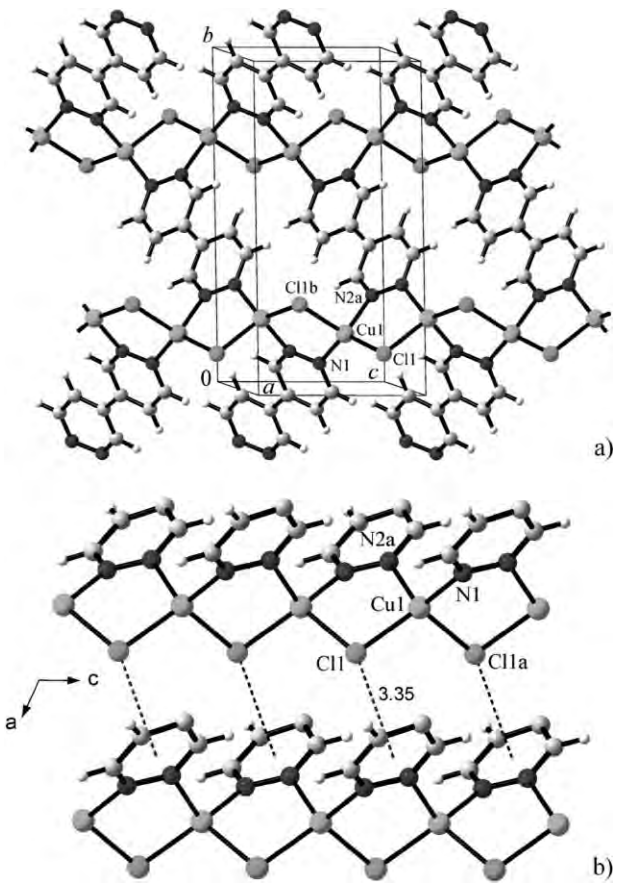


**Fig. 8** (a) 2D layered structure of isomorphous $Cu_2X_2$(4,4′-*bpdz*) complexes (X = Cl, Br) generated by tetradentate organic bridges and infinite $(CuX)_n$ chains, (b) complementary anion–π interactions between the successive layers.

**Table 4** Selected bond distances (Å) and angles (°) for complexes **7–9**

| | | | |
|---|---|---|---|
| $Cu_2Cl_2$(4,4′-*bpdz*) **7** (a: *x*, 1.5-*y*, −0.5+*z*; b: *x*, 1.5-*y*, 0.5+*z*) | | | |
| Cu1–N1 | 2.003(3) | N1–Cu1–N2a | 111.2(1) |
| Cu1–N2a | 2.087(3) | N1–Cu1–Cl1 | 124.23(9) |
| Cu1–Cl1 | 2.282(1) | N1–Cu1–Cl1b | 101.83(9) |
| Cu1–Cl1b | 2.375(1) | Cl1–Cu1–Cl1b | 110.98(6) |
| | | Cu1–Cl1–Cu1a | 92.80(4) |
| $Cu_2Br_2$(4,4′-*bpdz*) **8** (a: *x*, 1.5-*y*, −0.5+*z*; b: *x*, 1.5-*y*, 0.5+*z*) | | | |
| Cu1–N1 | 2.033(5) | N1–Cu1–N2a | 114.7(2) |
| Cu1–N2a | 2.076(5) | N1–Cu1–Br1 | 116.7(1) |
| Cu1–Br1 | 2.425(1) | N1–Cu1–Br1b | 102.8(1) |
| Cu1–Br1b | 2.470(1) | Br1–Cu1–Br1b | 113.23(5) |
| | | Cu1–Br1–Cu1a | 88.94(4) |
| $Cu_2I_2$(4,4′-*bpdz*) **9** (a: 0.5+*y*, 0.5-*x*, 0.25+*z*; b: 0.5-*y*, −0.5+*x*, −0.25+*z*) | | | |
| Cu1–N1 | 2.059(2) | N1–Cu1–N2a | 97.79(8) |
| Cu1–N2a | 2.097(2) | N1–Cu1–I1 | 112.82(5) |
| Cu1–I1 | 2.6047(4) | N2–Cu1–I1a | 104.11(5) |
| Cu1–I1b | 2.6185(4) | I1–Cu1–I1b | 118.26(1) |
| | | Cu1–I1–Cu1a | 78.69(1) |

In this context, it is should not be considered unusual that the iodide analog $Cu_2I_2$(4,4′-*bpdz*) **9** adopts a different, very remarkable 3D coordination pattern. There are no close iodine–π interactions. The inorganic portion of the structure exists as a four-fold helix $(CuI)_n$ with a pitch at 11.98 Å (parameter *c* of the unit cell) and the tetradentate organic bridges interconnect the helices into a 3D tetragonal framework (Fig. 9). Despite the significant length of the bipyridazine connector, the structure is not porous: a conformational flexibility of the ligand (dihedral angle between the cycles 34.7°) provides possibility for the "collapse" of the channels along the *c* direction and facilitates dense packing (Fig. 10).

For the complexes **7–9**, the higher electronegativity of the halogen atoms and the higher polarization of the $Cu^{I}$–X bonds favors effective σ-donor Cu–N coordination, which is reflected by a certain elongation of the Cu–N bonds in the bromide and the iodide *versus* the chloride compound (average Cu–N 2.055, 2.079 and 2.045 Å respectively, Table 4).

## Experimental

All chemicals were of analytical grade and were used as received without further purification. The copper(II) salt $CuS_2O_6 \cdot 6H_2O$ was prepared by ion exchange starting with barium dithionate. Hitherto unknown 4,4′-bipyridazine was easily accessible following the methodology of the "inverse electron demand Diels–Alder cycloadditons" of 1,2,4,5-tetrazine[26] and using inexpensive and available on a kilogram scale *cis*,*trans*-1,4-bis(dimethylamino)butadiene[27] as an extremely reactive "double dienophile" (scheme 3).

### 4,4′-Bipyridazine

Solution of 12.45 g (0.15 mol) 1,2,4,5-tetrazine in 150 mL of dry 1,4-dioxane was added dropwise for a period of 40 min to a stirred solution of 10.11 g (0.072 mol) of *cis*,*trans*-1,4-bis(dimethylamino)butadiene in 60 mL of dry 1,4-dioxane. The immediate evolution of nitrogen gas and discoloration were

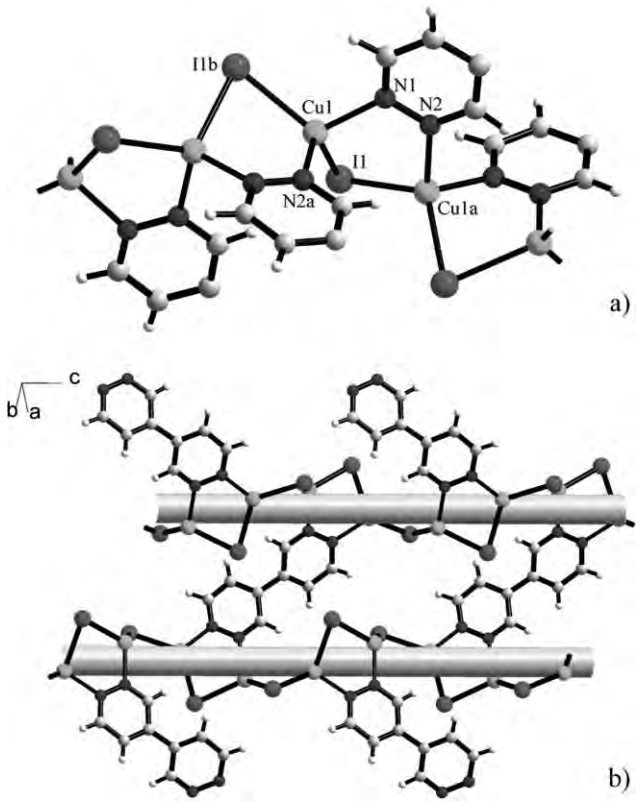


**Fig. 9** Coordination motif in the form of 1D pyridazino/cuproidide helix, which supports the structure of the 3D polymer **9** (a), interconnection of the neighboring $(CuI)_n$ helices with the tetradentate organic bridges (b).

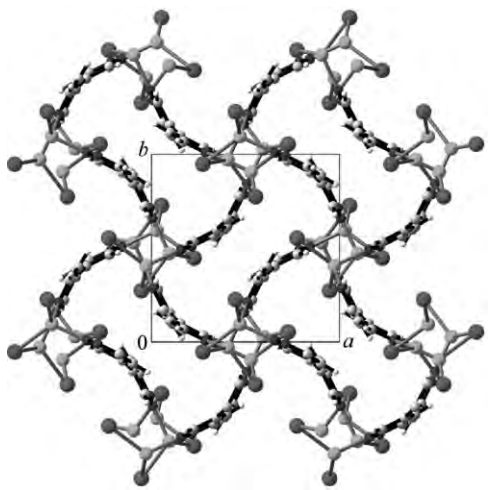


**Fig. 10** View of the structure of **9** along the direction of the cuproiodide helices illustrating "collapse" of the anticipated channels and formation of the densest packing.

accompanied with a pronounced exothermic effect. After the addition was completed, the red–brown reaction mixture was stirred at 80 °C for 4 h (elimination of dimethylamine) and then left overnight at r.t. The precipitate was filtered, washed with 5 mL $CH_2Cl_2$ and twice crystallized from methanol with charcoal yielding a pure product (4.44 g, 39%) as thin colorless needles. $^1$H-NMR (400 MHz, dmso-$D_6$, ppm) $\delta$: 9.77 (s, 2H, 3-CH), 9.37 (d, 2H, 6-CH), 8.23 (dd, 2CH, 5-CH). Anal. for $C_8H_6N_4$. Calc.

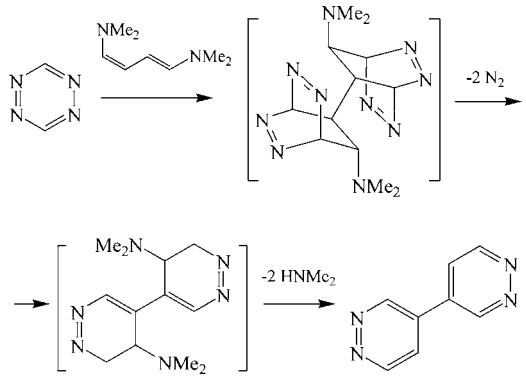


**Scheme 3** One-pot synthesis of 4,4′-bipyridazine involving cycloaddition and two-step elimination of nitrogen and dimethylamine.

(%): C, 60.75; H, 3.82; N, 35.43. Found (%): C, 60.44; H, 3.89; N, 35.17.

## Coordination compounds

**Preparation of Zn(4,4′-*bpdz*)$(NO_3)_2$ 2.** A solution of 0.030 g (0.1 mmol) of $Zn(NO_3)_2{\cdot}6H_2O$ in 2 mL methanol was layered over a solution of 0.016 g (0.1 mmol) of 4,4′-bipyridazine in a mixture of 2 mL methanol and 1 mL chloroform. Large colorless prisms of the complex (0.024 g, 70%) grew on the walls of the tube as the solutions slowly interdiffused in a 15 d period.

Anal. for **2**, $C_{16}H_{26}Cu_2N_4O_{12}$. Calc. (%): C, 32.38; H, 4.42; N, 9.44. Found (%): C, 32.12; H, 4.38; N, 9.16.

**Coordination compounds $Cu_2$(4,4′-*bpdz*)$(CH_3CO_2)_4{\cdot}4H_2O$ 1, $[Cu$(4,4′-*bpdz*$)_2(H_2O)_2]S_2O_6$ 3, $Cu_2$(4,4′-*bpdz*$)_3(CF_3CO_2)_4$ 4, and $[Cu_3$(4,4′-*bpdz*$)_6(H_2O)_4](BF_4)_6{\cdot}6H_2O$ 5.** These were prepared in 50–85% yields by slow evaporation of aqueous solutions of the components at r.t., while prolonged heating of the solutions may result in hydrolysis and crystallization of hydroxo compounds, as is illustrated in the following examples.

Anal. for **1**, $C_8H_6N_6O_6Zn$ (large green-blue prisms). Calc. (%): C, 27.64; H, 1.74; N, 24.19. Found (%): C, 27.48; H, 1.76; N, 24.03. For **3**, $C_{32}H_{18}Cu_2F_{12}N_{12}O_8$ (green prisms). Calc. (%): C, 36.47; H, 1.72; N, 15.96. Found (%): C, 36.21; H, 1.76; N, 15.80. For **4**, $C_{16}H_{16}CuN_8O_8S_2$ (deep-blue blocks). Calc. (%): C, 37.50; H, 3.15; N, 21.87. Found (%): C, 37.29; H, 3.07; N, 22.04. For **5**, $C_{48}H_{46}B_6Cu_3F_{24}N_{24}O_{10}$ (blue prisms). Calc. (%): C, 31.49; H, 2.53; N, 18.37. Found (%): C, 31.62; H, 2.40; N, 18.54.

**Preparation of $Cu_2$(4,4′-*bpdz*$)_3(CF_3CO_2)_4$ 4.** 0.039 g (0.1 mmol) of $Cu(CF_3CO_2)_2{\cdot}6H_2O$ and 0.016 g (0.1 mmol) of 4,4′-*bpdz* were dissolved in 2 ml water. Evaporation of the solution at r.t. over concentrated $H_2SO_4$ yields 0.030 g (85% based on the ligand) of the complex $Cu_2$(4,4′-*bpdz*$)_3(CF_3CO_2)_4$ **3**.

**Preparation of $[Cu_3(OH)_2$(4,4′-*bpdz*$)_3(H_2O)_2\{CF_3CO_2\}_2]$ $(CF_3CO_2)_2{\cdot}2H_2O$ 6.** 0.039 g (0.1 mmol) of $Cu(CF_3CO_2)_2{\cdot}6H_2O$ and 0.016 g (0.1 mmol) of 4,4′-*bpdz* were dissolved in 4 ml water and the solution was stirred in a 10 ml vial at nearly reflux temperature for 3 h. Several 1 ml portions of water were added during this period as the solution evaporated. The mixture was cooled and filtered. Slow evaporation at r.t. led to crystallization of the hydroxo complex **6**, as small grass-green prisms. The yield was 0.024 g (60%).

 

Anal. for **6**, $C_{32}H_{26}Cu_3F_{12}N_{12}O_{13}$. Calc. (%): C, 31.89; H, 2.17; N, 13.95. Found (%): C, 31.79; H, 2.23; N, 14.21.

**Copper(I) complexes 7–9.** These were prepared using a layering technique. In a typical synthesis, a solution of 0.038 g (0.2 mmol) of CuI in 3 ml acetonitrile was layered over a solution of 0.016 g (0.1 mmol) of the ligand in 3 ml of acetonitrile–chloroform mixture (2 : 1 v/v). Slow interdiffusion of the solutions led to a black crystalline product $Cu_2I_2$(4,4′-*bpdz*) **9** in 15 d. The yield was 0.043 g (80%). The chloride $Cu_2Cl_2$(4,4′-*bpdz*) **7** and bromide $Cu_2Br_2$(4,4′-*bpdz*) **8** (deep-red blocks) were prepared similarly using anhydrous acetonitrile and chloroform freshly distilled over $P_2O_5$.

Anal. for **7**, $C_8H_6Cl_2Cu_2N_4$. Calc. (%): C, 26.98; H, 1.70; N, 15.74. Found (%): C, 26.71; H, 1.77; N, 15.52. For **8**, $C_8H_6Br_2Cu_2N_4$. Calc. (%): C, 21.59; H, 1.36; N, 12.59. Found (%): C, 21.42; H, 1.42; N, 12.28. For **9**, $C_8H_6Cu_2I_2N_4$. Calc. (%): C, 17.82; H, 1.12; N, 10.40. Found (%): C, 17.69; H, 1.16; N, 10.31.

### Crystallography

Crystallographic measurements were made using a Stoe Imaging Plate Diffraction System for **1**, **3**, **5** and **6** (213 K, absorption corrections using DIFABS), Bruker APEX area-detector diffractometer for **2**, **4** and **9** (173 K, absorption corrections by SADABS[28]) and at r.t. using a four-circle Enraf Nonius CAD-4 diffractometer for **7** and **8** (absorption correction was based on psi-scans) (Mo-K$\alpha$ radiation, $\lambda = 0.71073$ Å). The structures were solved by direct methods using the program SHELXS-97.[29] The refinement and all further calculations were carried out using SHELXL-97.[29] The non-H atoms were refined anisotropically, using weighted full-matrix least-squares of $F^2$ (Table 5). For **2** and **9**, all hydrogen atoms were located and refined isotropically. For other structures CH hydrogens were added geometrically, OH hydrogen atoms were located and then fixed in structures **1**, **4** and **6**. For **5**, the hydrogen atoms of the water molecules were not located. In both trifluoroacetate structures **3** and **6**, the $CF_3$ groups shows typical rotational disorder, which was resolved with fixed geometry and with partial occupancies 0.5, 0.5 and 0.7, 0.3 (for two unique carboxylate anions in **3**) and 0.5, 0.5 in **6**. The disordered fluorine atoms were refined anisotropically for the sake of the overall convergence. One of the non-coordinated water molecules in structure **5** was equally disordered over two positions. Large anisotropy for thermal motion was also suggestive for possible disorder of one of the independent $BF_4^-$ anions. However, it was not possible to resolve the disordering scheme. No constraints in $BF_4^-$ geometry were applied. Graphical visualisation of the structures was made using the program Diamond.[30]

CCDC reference numbers 640632–640640.

For crystallographic data in CIF or other electronic format see DOI: 10.1039/b703911e

## Conclusions

The present study provides an efficient synthetic methodology and a very simple chemical access to 4,4′-bipyridazine as a novel polydentane N-donor for engineering network solids. The functional and conformational features of the ligand may be especially well suited for the development of highly connected coordination polymers and open frameworks, the design of polynuclear metal–organic clusters and their integration into the

**Table 5** Crystal data for $Cu_2$(4,4′-*bpdz*)$(CH_3CO_2)_4{\cdot}4H_2O$ **1**, Zn(4,4′-*bpdz*)$(NO_3)_2$ **2**, [Cu(4,4′-*bpdz*)$_2$$(H_2O)_2$]$S_2O_6$ **3**, $Cu_2$(4,4′-*bpdz*)$_3(CF_3CO_2)_4$ **4**, $[Cu_3(4,4'\text{-}bpdz)_6(H_2O)_4](BF_4)_6{\cdot}6H_2O$ **5**, $[Cu_3(OH)_2$(4,4′-*bpdz*)$_3$$(H_2O)_2\{(CF_3CO_2)_2\}_2]{\cdot}2H_2O$ **6**, $Cu_2Cl_2$(4,4′-*bpdz*) **7**, $Cu_2Br_2$(4,4′-*bpdz*) **8** and $Cu_2I_2$(4,4′-*bpdz*) **9**[a]

| | 1 | 2 | 3 | 4 | 5 | 6 | 7 | 8 | 9 |
|---|---|---|---|---|---|---|---|---|---|
| Formula | $C_{16}H_{26}Cu_2N_4O_{12}$ | $C_8H_6N_6O_6Zn$ | $C_{16}H_{16}CuN_8O_8S_2$ | $C_{32}H_{18}Cu_2F_{12}N_{12}O_8$ | $C_{48}H_{46}B_6Cu_3F_{24}N_{24}O_{10}$ | $C_{32}H_{26}Cu_3F_{12}N_{12}O_{13}$ | $C_8H_6Cl_2Cu_2N_4$ | $C_8H_6Br_2Cu_2N_4$ | $C_8H_6Cu_2I_2N_4$ |
| $M$ | 593.49 | 347.56 | 576.03 | 1053.66 | 1830.57 | 1205.27 | 356.15 | 445.07 | 539.05 |
| $T$/K | 213 | 173 | 213 | 173 | 213 | 213 | 293 | 293 | 213 |
| Crystal system | Triclinic | Monoclinic | Orthorhombic | Monoclinic | Monoclinic | Monoclinic | Monoclinic | Monoclinic | Tetragonal |
| Space group, $Z$ | $P\bar{1}$, 1 | $P2_1/n$, 4 | $Pna2_1$, 4 | $P2_1/c$, 2 | $P2/c$, 2 | $C2/c$, 4 | $P2_1/c$, 2 | $P2_1/c$, 2 | $P4_32_12$, 4 |
| $a$/Å | 7.4144(9); $\alpha = 76.96(1)°$ | 6.0750(1) | 15.106(1) | 10.4940(6) | 12.0861(8) | 15.4234(9) | 6.617(2) | 6.712(2) | 10.1405(5) |
| $b$/Å | 8.2275(9); $\beta = 82.51(1)°$ | 16.9431(3) | 11.8885(9) | 10.9798(8) | 14.6555(8) | 15.776(1) | 13.132(4) | 13.450(4) | 10.1405(5) |
| $c$/Å | 10.902(1); $\gamma = 63.27(1)°$ | 11.9592(2) | 11.063(1) | 18.306(1) | 21.567(1) | 19.103(1) | 6.642(2) | 6.807(3) | 11.9784(7) |
| $\beta$/° | | 101.380(1) | | 98.572(5) | 104.025(8) | 108.591(6) | 114.23(2) | 112.79(3) | |
| $U$/Å$^3$ | 578.35(14) | 1206.75(4) | 1986.9(3) | 2085.7(2) | 3706.3(4) | 4405.7(5) | 526.3(3) | 566.6(3) | 1231.7(1) |
| $\mu$(Mo-K$\alpha$)/mm$^{-1}$ | 1.907 | 2.078 | 1.380 | 1.137 | 0.982 | 1.562 | 4.518 | 10.779 | 8.441 |
| $D_c$/g cm$^{-3}$ | 1.704 | 1.913 | 1.926 | 1.678 | 1.640 | 1.817 | 2.247 | 2.609 | 2.907 |
| $\theta_{max}$/° | 28.08 | 28.70 | 28.08 | 27.88 | 26.55 | 27.00 | 24.97 | 24.99 | 27.97 |
| Meas/Unique refins | 6716/2758 | 7745/3070 | 14287/4759 | 10418/4887 | 12405/7639 | 11224/4587 | 1003/923 | 1068/983 | 11901/1478 |
| $R_{int}$ | 0.030 | 0.028 | 0.046 | 0.030 | 0.046 | 0.051 | 0.031 | 0.076 | 0.038 |
| Parameters refined | 154 | 214 | 317 | 352 | 529 | 385 | 73 | 73 | 85 |
| $R1$, $wR2$ [$I > 2\sigma(I)$] | 0.027, 0.074 | 0.028, 0.067 | 0.044, 0.105 | 0.043, 0.104 | 0.059, 0.157 | 0.036, 0.093 | 0.032, 0.085 | 0.038, 0.093 | 0.012, 0.024[a] |
| Goof on $F^2$ | 1.061 | 1.054 | 1.048 | 1.035 | 0.943 | 0.983 | 1.073 | 1.050 | 0.966 |
| Max, min peak/$e$ Å$^{-3}$ | 0.42, −0.39 | 0.30, −0.37 | 0.79, −0.48 | 0.50, −0.41 | 0.98, −0.56 | 0.74, −0.40 | 0.38, −0.43 | 0.97, −0.60 | 0.44, −0.28 |

[a] Flack parameter $x = 0.01(2)$.

extended structure. Coordination preferences of the ligand and its affinity towards "soft" Cu(I) cations allows rational approaches towards novel hybrid organic/inorganic materials incorporating typical inorganic motifs bridged by pyridazine. Our results suggest that the weak anion–π interactions, which are known entirely for the most electron deficient heterocycles, may also be relevant for the pyridazine derivatives as a factor for controlling the supramolecular structure.

## Acknowledgements

The work was in part supported by a grant from Deutsche Forschungsgemeinschaft UKR 17/1/06 (HK and KVD).

## References

1 C. Janiak, *Dalton Trans.*, 2003, 2781; C. J. Kepert, *Chem. Commun.*, 2006, 695; S. Kitagawa, S. Noro and T. Nakamura, *Chem. Commun.*, 2006, 701.
2 M. Eddaoudi, D. B. Moler, H. Li, B. Chen, T. M. Reineke, M. O'Keeffe and O. M. Yaghi, *Acc. Chem. Res.*, 2001, **34**, 319; A. Y. Robin and K. M. Fromm, *Coord. Chem. Rev.*, 2006, **250**, 2127.
3 B. Moulton and M. J. Zaworotko, *Chem. Rev.*, 2001, **101**, 1629.
4 C. J. Elsevier, J. Reedijk, P. H. Walton and M. D. Ward, *Dalton Trans.*, 2003, 1869; A. N. Khlobystov, A. J. Blake, N. R. Champness, D. A. Lemenovskii, A. G. Majouga, N. V. Zyk and M. Schröder, *Coord. Chem. Rev.*, 2001, **222**, 155.
5 M. Casarin, C. Corvaja, C. Di Nicola, D. Falcomer, L. Franco, M. Monari, L. Pandolfo, C. Pettinari and F. Piccinelli, *Inorg. Chem.*, 2005, **44**, 6265; C. D. Nicola, Y. Y. Karabach, A. M. Kirillov, M. Monari, L. Pandolfo, C. Pettinari and A. J. Pombeiro, *Inorg. Chem.*, 2007, **46**, 221.
6 J. He, Y. G. Yin, T. Wu, D. Li and X. C. Huang, *Chem. Commun.*, 2006, 2845.
7 Y. Mulyana, C. J. Kepert, L. F. Lindoy, A. Parkin and P. Turner, *Dalton Trans.*, 2005, 1598.
8 A. B. Lysenko, E. V. Govor, H. Krautscheid and K. V. Domasevitch, *Dalton Trans.*, 2006, 3772; A. B. Lysenko, E. V. Govor and K. V. Domasevitch, *Inorg. Chim. Acta*, 2007, **360**, 55.
9 L. Plasseraud, H. Maid, F. Hampel and R. W. Saalfrank, *Chem.–Eur. J.*, 2001, **7**, 4007; L. Carlucci, G. Ciani, D. M. Proserpio and A. Sironi, *Inorg. Chem.*, 1998, **37**, 5941.
10 T. Otieno, S. J. Rettig, R. C. Thompson and J. Trotter, *Inorg. Chem.*, 1995, **34**, 1718; L. Carlucci, G. Ciani, M. Moret and A. Sironi, *J. Chem. Soc., Dalton Trans.*, 1994, 2397.
11 H.-Y. Bie, J.-H. Yu, K. Zhao, K. Lu, L.-M. Duan and J.-Q. Xu, *J. Mol. Struct.*, 2005, **741**, 77.
12 J. Tao, Z. J. Ma, R. B. Huang and L. S. Zheng, *Inorg. Chem.*, 2004, **43**, 6133.
13 M. Kondo, M. Shimamura, S. Noro, T. Yoshitomi, S. Minakoshi and S. Kitagawa, *Chem. Lett.*, 1999, 285.
14 R.-G. Xiong, B. J. Lewandowski and S. D. Huang, *Z. Kristallogr. –New Cryst. Struct.*, 1999, **214**, 461.
15 B. L. Schottel, J. Basca and K. R. Dunbar, *Chem. Commun.*, 2005, 46; B. L. Schottel, H. T. Chifotides, M. Shatruk, A. Chouai, L. M. Perez, J. Bacsa and K. R. Dunbar, *J. Am. Chem. Soc.*, 2006, **128**, 5895.
16 P. U. Maheswari, B. Modec, A. Pevec, B. Kozlevčar, C. Massera, P. Gamez and J. Reedijk, *Inorg. Chem.*, 2006, **45**, 6637; H. Casellas, C. Massera, F. Buda, P. Gamez and J. Reedijk, *New J. Chem.*, 2006, **30**, 1561.
17 I. A. Gural'skiy, P. V. Solntsev, H. Krautscheid and K. V. Domasevitch, *Chem. Commun.*, 2006, 4808.
18 S. R. Batten and R. Robson, *Angew. Chem., Int. Ed.*, 1998, **37**, 1460; S. R. Batten, *CrystEngComm*, 2001, **3**, 67.
19 M. J. Zaworotko, *Chem. Commun.*, 2001, 1.
20 S. Noro, R. Kitaura, M. Kondo, S. Kitagawa, T. Ishii, H. Matsuzaka and M. Yamashita, *J. Am. Chem. Soc.*, 2002, **124**, 2568.
21 A. Neels, M. Alfonso, D. G. Mantero and H. Stoeckli-Evans, *Chimia*, 2003, **57**, 619.
22 C. Nather and I. Jess, *Inorg. Chem.*, 2003, **42**, 2968; P. C. Healy, J. D. Kildea, B. W. Skelton and A. H. White, *Aust. J. Chem.*, 1989, **42**, 79.
23 G. S. Chandler, C. L. Raston, G. W. Walker and A. H. White, *J. Chem. Soc., Dalton Trans.*, 1974, 1797.
24 P. V. Solntsev, J. Sieler, H. Krautscheid and K. V. Domasevitch, *Dalton Trans.*, 2004, 1153.
25 S. Demeshko, S. Dechert and F. Meyer, *J. Am. Chem. Soc.*, 2004, **126**, 4508; M. Mascal, A. Armstrong and M. D. Bartberger, *J. Am. Chem. Soc.*, 2002, **124**, 6274.
26 A. T. M. Marcelis and H. C. von der Plas, *J. Heterocycl. Chem.*, 1987, **24**, 545; J. Sauer, D. K. Heldmann, J. Hetzenegger, J. Krauthan, H. Sichert and J. Schuster, *Eur. J. Org. Chem.*, 1998, 2885.
27 M. F. Fegley, N. M. Bortnick and C. H. McKeever, *J. Am. Chem. Soc.*, 1958, **79**, 4140.
28 G. M. Sheldrick, *SADABS Area-Detector Absorption Correction, 2.03*, University of Göttingen, Germany, 1999.
29 G. M. Sheldrick, *SHELXS-97 & SHELXL-97, Computer programs for the solution and refinement of X-ray crystal structures*, University of Göttingen, Germany, 1997.
30 K. Brandenburg, *Diamond 2.1c*, Crystal Impact GbR, Bonn, 1999.

 